JOURNAL OF SOLID STATE CHEMISTRY 100, 255–261 (1992)

Crystal Structure of Neodymium-Ion-Exchanged β-Alumina

F. TIETZ AND W. URLAND

Institut für Anorganische Chemie der Universität Hannover and Sonderforschungsbereich 173, Callinstr. 9, D-3000 Hannover 1, Germany

Received March 12, 1992; accepted March 14, 1992

The structure of a neodymium-exchanged Na^+-β-alumina crystal ($P6_3/mmc$, $Z = 2$, $a = 5.5848(8)$ Å, $c = 22.406(5)$ Å) with the analytical composition $Na_{0.08}Nd_{0.38}Al_{11}O_{17.10}$ has been investigated by conventional X-ray diffraction methods at room temperature. The refinement ($R = 0.0653$, $R_w = 0.0446$) shows a highly disordered ion distribution in the conduction planes due to the high coulombic force of the Nd^{3+} ions which are preferentially located at BR sites. Structural properties are discussed in comparison with other crystal structure determinations of β-alumina isomorphs published recently.
© 1992 Academic Press, Inc.

1. Introduction

During the last 20 years the crystal chemistry of Na^+–β-alumina, the prototype of a two-dimensional sodium ion conductor, has been investigated (*1, 2*) and the conduction mechanism is understood quite well by now (*3–6*). Because of the high mobility of the sodium ions it is possible to carry out ion exchange using molten salts of monovalent (*7*) or divalent (*7, 8*) cations. The latter show very slow diffusion rates (*7*) and the only readily exchangeable divalent ion is Cd^{2+} (*8, 9*). Highly Cd^{2+}-exchanged β-alumina has a poor ionic conductivity and a high activation energy (*9*). The Cd^{2+} ions occupy 6*h* sites (space group $P6_3/mmc$) within the conduction planes close to the so-called mid-oxygen (mO) sites (*10–13*).

Although there are difficulties to incorporate divalent cations into the β-Al_2O_3 structure, we successfully carried out ion exchange (up to 95%) with lanthanide ions (*14*). Very recently rare earth ions could also be incorporated into β-aluminogallates (*15*). Here we present the crystal structure of a 93% ion-exchanged Na^+/Nd^{3+}–β-Al_2O_3 single crystal, having the composition $Na_{0.08\pm0.01}Nd_{0.38\pm0.03}Al_{11\pm0.03}O_{17.10\pm0.10}$ and the hexagonal cell parameters $a = 5.5848(8)$ Å and $c = 22.406(5)$ Å.

2. Experimental

Commercially available crystals (Ceramatec, Inc.) were ion exchanged (*14*) and analyzed (*16*) as described previously. A small and optically clear crystal was cut from a larger parent crystal and used for X-ray diffraction studies.

X-ray photography was carried out using a Huber precession camera. The intensity measurements were performed at room temperature with a four circle diffractometer (AED 2, Siemens–Stoe). The experimental data are listed in Table I.

0022-4596/92 $5.00
Copyright © 1992 by Academic Press, Inc.
All rights of reproduction in any form reserved.

TABLE I

EXPERIMENTAL PARAMETERS RELATING TO THE DATA COLLECTION AND REFINEMENT OF $Na_{0.08}Nd_{0.38}Al_{11}O_{17.10}$

Cell parameters (298 K)	a = 5.5848(8) Å, c = 22.406(5) Å
Cell volume (298 K)	605.2(3) Å^3
Formula units per unit cell	2
ρ (X-ray)	3.44 g · cm^{-3}
Space group	$P6_3/mmc$
Crystal dimensions	(0.28 × 0.088 × 0.035) mm^3
Four circle diffractometer	Siemens–Stoe AED 2
Radiation	Mo-K_α (graphite-monochromator)
Intensity measurement method	ω-2Θ-scan
Degree intervals per step	variable, "learnt profile method," Ref. (18)
Time intervals per stop	0.5–1.0 sec
Standard reflections	$\bar{4}\,2\,0$, $\bar{2}\,2\,\bar{13}$, 3 0 4
Intensity variations	±6.85%
2Θ range	2°–60°
Min./max. sin Θ/λ	0.0446/0.7021 Å^{-1}
h, k, l range	$\bar{8}$, $\bar{8}$, $\bar{32}$ to 0, 8, 32
No. of observed reflexes	3815
No. of unique reflexes	393
No. of reflexes with $F_o \geq 3\sigma(F_o)$	389
R_{int}	0.0629
Min./max. transmission factor	0.5287/0.9137
Linear absorption factor	25.79 cm^{-1}
Refined parameters	57
Absorption correction	Numerical
Method of structure refinement	Starting parameters for spinel block atoms from Ref. (*1*), atoms with z = 0.25 from difference Fourier syntheses
R, R_w	0.0653, 0.0446
Max./min. peak in final difference map	1.36/−0.99 e · Å^{-3}
Max. $\lvert\Delta\rvert/\sigma$	0.011
Program used	SHELX-76

3. Results

The precession photographs showed a hexagonal symmetry with systematic absences indicating the possible space groups $P6_3/mmc$ or $P6_3mc$. In the diffraction patterns of the sheets [hk0], [hk1], and [hk2] weak reflections indicate a commensurate superstructure with a $3a \times 3a$ supercell. Because of their very low intensities they were not included in the diffractometer measurements. The final atomic parameters, the anisotropic displacement factors for the atoms in the conduction plane and the interatomic distances are listed in Tables II, III, and IV, respectively.

4. Refinements

Starting parameters for the refinement of the spinel block atoms were taken from Ref. (*1*). The resulting electron density map of a difference Fourier synthesis of the conduction plane shows a strong maximum in the 2d site (Beevers–Ross (BR) site) and a highly disordered O(5) atom (Fig. 1a). Further, it is interesting to note that no electron density is found in the mO site. Therefore, Nd^{3+} was located at the BR site and a split position for the column-oxygen O(5) was introduced. Hereafter the split positions are referred to as O(51) (dislocated in direction to the BR site) and O(52) (shifted toward the anti-Beevers–Ross (aBR) site, Figs. 1a–1c).

After introducing the anisotropic displacement parameters the small residual electron density peaks in the aBR and near the BR site were included in the refinement procedure. Attempts were made to test the noncentrosymmetric space group $P6_3mc$ and also to constrain the occupation parameters to the analytical contents for Nd^{3+} as well as for O(51) and O(52), but no improvement of the parameters was found. We tried to locate the sodium ions anywhere along the conduction pathways, but the obtained coordinates and displacement parameters were not reliable and physically unreasonable. Hence the small electron density peaks were firstly also occupied with neodymium and refined isotropically leading to a slight

TABLE II

SITE MULTIPLICITIES, OCCUPATION FACTORS, AND FRACTIONAL ATOMIC COORDINATES ($y = -x$) FOR $Na_{0.08}Nd_{0.38}Al_{11}O_{17.10}$

Atom	Site	Occupation factor	x	z
Nd(1)	2*d*	0.320(5)	$\frac{2}{3}$	$\frac{1}{4}$
Nd(2)	6*h*	0.017(2)	−0.231(7)	$\frac{1}{4}$
Na	2*b*	0.064(2)	0	$\frac{1}{4}$
$Al_{int.}$	2*b*	0.040(8)	0	$\frac{1}{4}$
Al(1)	12*k*	1.0	−0.1678(2)	0.1077(1)
Al(2)	4*f*	1.0	$\frac{1}{3}$	0.0248(1)
Al(3)	4*f*	0.960(8)	$\frac{1}{3}$	0.1776(1)
Al(4)	2*a*	1.0	0	0
O(1)	12*k*	1.0	0.1573(4)	0.0502(1)
O(2)	12*k*	1.0	0.5032(4)	0.1477(1)
O(3)	4*f*	1.0	$\frac{2}{3}$	0.0562(2)
O(4)	4*e*	1.0	0	0.1427(3)
O(51)	6*h*	0.30(1)	0.392(2)	$\frac{1}{4}$
O(52)	6*h*	0.12(1)	0.180(5)	$\frac{1}{4}$

Note. The standard deviations are shown in parentheses.

excess of the total Nd^{3+}, O(51), and O(52) occupation with respect to the analytical composition. Also from a structural point of view the fivefold coordination of Nd^{3+} at the aBR site is very unsatisfactory. Therefore, with regard to the similar oxygen positions

TABLE III

ISOTROPIC (U_{iso}), ANISOTROPIC DISPLACEMENT PARAMETERS (U_{ij}) FOR THE Na^+, Nd^{3+}, AND O(5) POSITIONS AND EQUIVALENT ISOTROPIC DISPLACEMENT PARAMETERS ($U_{eq} = \frac{1}{3}[U_{33} + \frac{4}{3}(U_{11} + U_{22} - U_{12})]$) (*19*) FOR THE SPINEL BLOCK ATOMS (Å^2)

Atom	U_{11}	U_{22}	U_{33}	U_{iso}
Nd(1)	0.016(1)	U_{11}	0.024(1)	—
Nd(2)	—	—	—	0.078(10)
Na/Alint.	—	—	—	0.016(9)
O(51)	0.034(9)	0.011(9)	0.005(6)	—
O(52)	0.021(10)	0.047(11)	0.010(10)	—
	$U_{12} = 0.5 \times U_{22}$, $U_{13} = U_{23} = 0$			
				U_{eq}
Al(1)				0.0109(7)
Al(2)				0.0075(7)
Al(3)				0.0104(8)
Al(4)				0.0087(10)
O(1)				0.008(2)
O(2)				0.009(2)
O(3)				0.008(1)
O(4)				0.010(2)

TABLE IV

INTERATOMIC DISTANCES (Å) IN $Na_{0.08}Nd_{0.38}Al_{11}O_{17.10}$

Na(1)–O(2)	2.785(3)	Al(1)–O(1)	2.034(3)
Nd(1)–O(51)	2.662(9)	Al(1)–O(2)	1.828(3)
Nd(1)–O(52)	2.80(3)	Al(1)–O(3)	1.974(4)
$Na/Al_{int.}$–O(4)	2.405(6)	Al(1)–O(2)	1.802(3)
Na–O(51)	2.983(9)	Al(2)–O(1)	1.796(3)
$Na/Al_{int.}$–O(52)	1.74(2)	Al(2)–O(2)	1.815(6)
Nd(2)–O(2)	2.68(1)	Al(3)–O(2)	1.773(3)
Nd(2)–O(4)	3.28(3)	Al(3)–O(51)	1.718(4)
Nd(2)–O(51)	2.33(3)	Al(3)–O(52)	2.20(2)
Nd(2)–O(52)	2.92(4)	Al(4)–O(1)	1.893(3)

of O(52) and the oxygen in the mirror plane of the magnetoplumbite-type structure (c.f. Figs. 1b and 1d) we tried to introduce Al^{3+} ions in the aBR site. These aluminum ions can come only from neighboring sites near the conduction layers. Because of this, the refinement of the occupation factor of the interstitial Al^{3+} in the aBR site was constrained to the decreasing occupation factor of Al(3). After this step, a small electron density was still found in the aBR site and together with the aluminium ions the sodium content could now also be refined.

The interstitial Al atoms in 12*k* sites forming the Roth–Reidinger defect and normally stabilizing the additional oxygen in the conduction layers (*2, 17*) could not be located, no more than could the interstitial oxygen which is usually found in mO sites. On the other hand, the sum of the O(51) and O(52) occupation yields an excess oxygen content which was always in the range of about 0.3–0.5 O^{2-} ions per unit cell.

5. Discussion

The neodymium ions show a high preference for the BR site and because of the shift of the O(51) ions they achieve an eight- or ninefold coordination, as usually found for the early lanthanide ions. The final refined composition of the crystal is $Na_{0.06}Nd_{0.37}Al_{11}O_{17.26}$ with an excess of negative charge of 0.7 e^- per unit cell. Taking the more faulty parameters of O(51) and O(52) into account and constraining the occupation factors of these ions to 90% of the refined value, the analytical composition would exactly be achieved.

The structure of Na^+–β-Al_2O_3 is built up by spinel blocks separated in the *c* direction by Al(3)–O(5)–Al(3) columns which form bridges perpendicular to the conduction planes (*1*). After the ion exchange the investigated Nd^{3+}–β-Al_2O_3 shows a strong deformation of this brigding unit (Fig. 2). The bond angle of Al(3)–O(51)–Al(3) is now 141.8°, the O(51) ions are strongly dislocated due to the coulombic attraction of the Nd^{3+} ions. Moreover, the O(52) ions show a much stronger dislocation and the bond angle between two Al(3) ions is 95.0°.

To explain this dislocation we have to consider a possible arrangement in a $3a \times 3a$ supercell, which is indeed favored considering to the precession photographs. For attaining a nearly analytical composition we have to fill up the conduction plane of this enlarged cell with 1 Na^+ and 3 Nd^{3+} ions as well as 10 oxygen ions. The three Nd^{3+} ions are positioned on BR sites and eight of the 10 O(5) oxygens stabilize the Nd^{3+} ions on O(51) positions. Taking many possible arrangements two neighboring unit cells are occupied with Nd^{3+} ions. In this situation an O(52) ion, positioned nearly in the middle

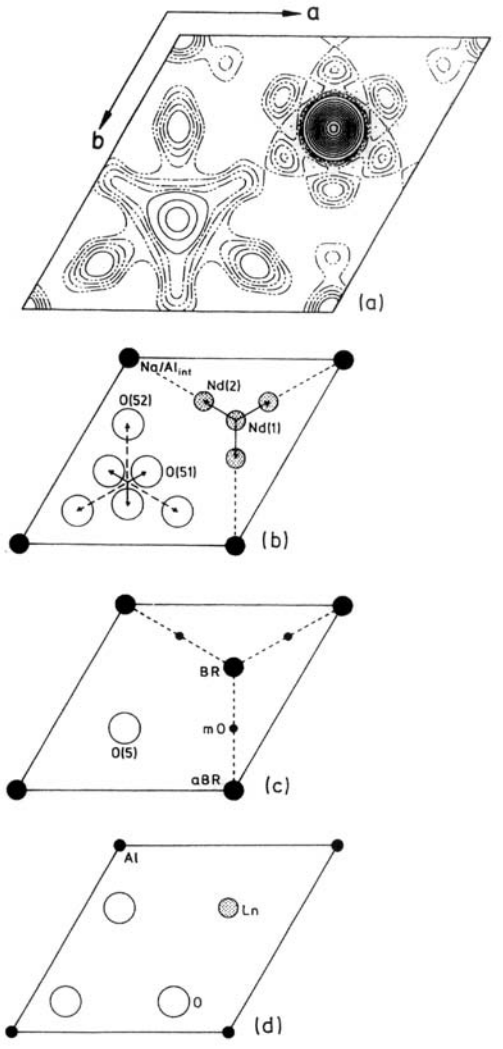

FIG. 1. (a) Electron density map of the conduction plane of $Na_{0.08}Nd_{0.38}Al_{11}O_{17.10}$. The contour intervals are 1 eÅ^{-3}. For the dashed lines the contour interval is 0.25 eÅ^{-3} finishing at the zero level. (b) A schematic representation of the sites occupied in $Na_{0.08}Nd_{0.38}Al_{11}O_{17.10}$, (c) of the most important sites in the conduction plane ($z = 0.25$) of β-Al_2O_3, and (d) of the mirror plane ($z = 0.25$) in the magnetoplumbite type structure.

between these two neodymiums, can give the best stabilization. The shortest distance to another O(52) site is 2.57 Å, somewhat shorter than $O(5)$–$O_{interstitial(mO)}$ $(a/2) \approx 2.8$ Å in the case of the Roth-Reidinger defect (*17*). Therefore it is possible that in one unit cell two O(52) ions can reside. Following this train of thought we can regard the O(52) ions to be interstitial and stabilizing. This explains not only the low site occupancy but also other effects:

—the disappearance of interstitial oxygens in the mO site or, in general, the disappearance of the stabilization by the Roth–Reidinger defect as mentioned in Ref. (*14*),

—the change of the observed differences in stoichiometry after ion exchange at different temperatures (*14*) due to the enhanced mobility of the oxygen ions in the conduction planes,

—the possible degradation of highly exchanged lanthanide β-alumina crystals. Sometimes β-Al_2O_3 crystals look pale after ion exchange. It can be assumed that these crystals partially adopt the magnetoplumbite type structure (*20*). In this structure the oxygen atoms in the mirror plane ($z = 0.25$) have nearly the same positions as O(52) (c.f. Table V) and aluminium atoms are located in the β-alumina analogous aBR site (Figs. 1c and 1d). Indeed, although we did not finally refine the aBR position anisotropically, this site shows a strong vibrational amplitude in the c direction.

However, keeping this in mind the investigated crystal seems to show a possible way for a decomposition mechanism. This extreme situation can also be discussed with more general aspects following the schemes of Iyi *et al.* (*21*). The authors define the thickness of the conduction layer to be the

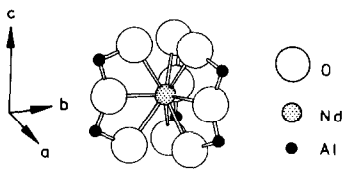

FIG. 2. Coordination sphere of an Nd^{3+} ion at a BR site.

TABLE V

STRUCTURAL CHARACTERISTICS FOR VARIOUS β-ALUMINA COMPOUNDS

Compound	Cond. plane thickness (Å)	Spinel block thickness (Å)	Al(3)–O(5) distance (Å)	O(5) in (2c)	O(5) in (6h)[a]	c/a	Ref.
Na^+–β-Al_2O_3	4.65	6.61	1.677	2c	—	4.03	(1)
Na^+–β-Al_2O_3	4.67	6.59	1.672	2c	—	4.03	(2)
Ag^+–β-Al_2O_3	4.65	6.57	1.666	2c	—	4.01	(10)
Na^+/Cd^{2+}–β-Al_2O_3[d]	4.61	6.60	1.664	2c	0.60[b]	4.01	(12)
Cd^{2+}–β-$(Al,Mg)_2O_3$				—	0.56[b]	3.95	(11)
Cd^{2+}–β-Al_2O_3	4.62	6.57	1.735	—	0.54[b]	4.00	(13)
Na^+/Nd^{3+}–β-$(Al,Ga)_2O_3$[e]	4.63	6.68	1.700	—	0.45[c]	4.01	(15)
Na^+/Nd^{3+}–β-Al_2O_3[f]	4.58	6.62	1.718/2.20	—	0.56[c]/1.48[b]	4.01	This work
$LaMgAl_{11}O_{19}$	4.37	6.64	1.974		1.46[b,g]	3.94	(20)

Note. For comparison, values are added for $LaMgAl_{11}O_{19}$ crystallizing in the magnetoplumbite type structure.

[a] Shifted from 2c site by the given values (in Å).

[b] Direction of the shift as defined for O(52) in the text.

[c] Direction of the shift as defined for O(51) in the text.

[d] Exchange rate 79%.

[e] Exchange rate 50%.

[f] Exchange rate 93%.

[g] Theoretical shift from $\frac{1}{3}$, $\frac{2}{3}$, $\frac{1}{4}$ to 0.182, 0.818, $\frac{1}{4}$ (20).

distance between two opposite interspinel block O(2) ions ($[(0.5 - z_{(O2)}) - z_{(O2)}] \times c$) and the thickness of the spinel block to be the intraspinel block O(2)–O(2) distance ($[(0.5 + z_{(O2)}) - (0.5 - z_{(O2)})] \times c$). Using these definitions we calculated the conduction layer thickness, the spinel block thickness, and the O(5) dislocations. The corresponding values together with the c/a ratio and the Al(3)–O(5) distances of recently published data for various β-aluminas are listed in Table V.

In the case of the conduction layer thickness, all reported values except the one of this work are larger than 4.6 Å, which is said to be the lower limit for β-alumina. Below this limit there is the stability region of the magnetoplumbite type structure (*21*). A conduction layer thickness of 4.58 Å is not only the smallest ever reported, it seems to be the absolute limit for this structure type. Assuming an ideal O(5) position at the 2c site the Al(3)–O(5) distance would be only 1.624 Å. This is too short and a shift to a 6c site is the logical consequence. Another limit is reached in the case of the c/a ratio. For Nd^{3+}, as well as for Cd^{2+}–β-alumina, the c/a ratio of 4.00–4.01 seems to be the smallest value (*21, 22*). Only Boilot *et al.* achieved a lower value using Mg^{2+}-stabilized β-alumina (*11*).

Iyi *et al.* (*21*) mentioned an increase of the spinel block thickness due to Al^{3+} vacancies in the Al(1) site. All listed compounds in Table V are within the range of 0–0.5 Al^{3+} defects per unit cell and show no significant change in the spinel block thickness. The reason for the enlarged value for the β-aluminogallate is the incorporation of larger Ga^{3+} ions for Al^{3+} ions.

6. Conclusions

This work gives some insights into the crystal chemistry of lanthanide-ion-exchanged β-aluminas. The trivalent ions are

preferentially located at BR sites. The rest could be found about 1 Å apart from this site along the conduction pathways. Because of the high coulombic interaction of the Nd^{3+} ions the column-oxygens show a high disorder and are dislocated from their original position up to 1.5 Å. This can be interpreted in terms of a stabilization mechanism and to be the first step of a rearrangement to adopt the magnetoplumbite structure. Also the small conduction layer thickness indicate the beginning of a structure degradation as well. High-resolution electron microscopy could give more detailed information about the atomic rearrangements at pathological crystal domains.

Acknowledgments

We thank Dr. J. Koepke for the analytical measurements and the Deutsche Forschungsgemeinschaft for financial support.

References

1. C. R. Peters, M. Bettman, J. W. Moore, and M. D. Glick, *Acta Crystallogr., Sect. B* **27,** 1826 (1971).
2. K. Edström, J. O. Thomas, and G. C. Farrington, *Acta Crystallogr., Sect. B* **47,** 210 (1991).
3. K. K. Kim, J. N. Mundy, and W. K. Chen, *J. Phys. Chem. Solids* **40,** 743 (1979).
4. D. Wolf, *J. Phys. Chem. Solids* **40,** 757 (1979).
5. J. R. Walker and C. R. A. Catlow, *J. Phys. C: Solid State Phys.* **15,** 6151 (1982).
6. J. F. Bocquet and G. Lucazeau, *Solid State Ionics,* **24,** 235 (1987).
7. Y.-F. Y. Yao and J. T. Kummer, *J. Inorg. Nucl. Chem.* **29,** 2453 (1967).
8. G. C. Farrington and B. Dunn, *Solid State Ionics* **7,** 267 (1982).
9. P. H. Sutter, L. Cratty, M. Saltzberg, and G. C. Farrington, *Solid State Ionics* **9 & 10,** 295 (1983).
10. K. Edström, J. O. Thomas, and G. C. Farrington, *Acta Crystallogr., Sect. B* **47,** 643 (1991).
11. J. P. Boilot, P. Colomban, and M. R. Lee, *Solid State Ionics* **9 & 10,** 315 (1983).
12. M. Catti, E. Cazzanelli, G. Ivaldi, and G. Mariotto, *Phys. Rev. B* **36,** 9451 (1987).
13. K. Edström, J. O. Thomas, and G. C. Farrington, *Acta Crystallogr., Sect. B* **47,** 635 (1991).
14. F. Tietz and W. Urland, *Solid State Ionics* **46,** 331 (1991).
15. A. Kahn-Harari, G. Aka, and J. Théry, *J. Solid State Chem.* **91,** 71 (1991).
16. F. Tietz, J. Koepke, W. Urland, *J. Crystal Growth* **118,** 314 (1992).
17. W. L. Roth, F. Reidinger, S. Laplaca, *in* "Superionic Conductors" (G. D. Mahan, W. L. Roth, Eds.), p. 223, Plenum Press, New York (1976).
18. W. Clegg, *Acta Crystallogr., Sect. A* **37,** 22 (1981).
19. R. X. Fischer and E. Tillmanns, *Acta Crystallogr., Sect. C* **44,** 775 (1988).
20. A. Kahn, A. M. Lejus, M. Madsac, J. Théry, and D. Vivien, *J. Appl. Phys.* **52,** 6864 (1981).
21. N. Iyi, S. Takekawa, and S. Kimura, *J. Solid State Chem.* **83,** 8 (1989).
22. J. M. P. J. Verstegen and A. L. N. Stevels, *J. Lumin.* **9,** 406 (1974).